Corrugated waveguides as resonance optical filters—advantages and limitations

Evgeny Popov

Case 262, Institut Fresnel, Unité Mixte de Recherche, Centre National de la Recherche Scientifique 6133, Faculté des Sciences de St. Jèrôme, Avenue Escadrille Normandie-Niemen, 13397 Marseille Cedex 20, France

Bozhan Bozhkov

Institute of Solid State Physics, 72 Tzarigradsko Chaussee Boulevard, 1784 Sofía, Bulgaria

Received July 28, 2000; revised manuscript received November 13, 2000; accepted November 15, 2000

The role of the excitation of guided waves propagating in a corrugated dielectric waveguide is discussed in view of the resonance anomalies in reflectivity. Narrow-wavelength filtering properties that are due to these sharp anomalies have been a topic of interest for some time, but a proper understanding of device performances requires an analysis of tolerances with respect to the incident-beam collimation and to waveguide losses. Such an analysis is proposed in this paper, and the conclusion is that the incident-beam divergence plays a critical role in reducing the maximum reflectivity for narrow-band filters. © 2001 Optical Society of America

OCIS codes: 050.1950, 230.7370.

1. HISTORICAL REVIEW

The first observation of sharp changes in the diffraction efficiency of diffraction gratings was made by Wood[1] in 1902. To him is due the credit for the name "anomaly" that was given to this phenomenon. Much later, in 1950, Fano[2] was the first to distinguish between resonant and nonresonant anomalies, the former because of the excitation of guided waves and the latter appearing when some diffraction order is being passed off. In 1964, Hessel and Oliner[3] proposed a phenomenological approach to resonant anomalies that introduces the poles and the zeros of the diffraction efficiency. The pole appears because of guided-wave excitation. In brief, it is the result of the solution of the homogeneous problem when a guided wave exists without an incident wave. This solution requires that the scattering matrix that links the diffracted- and the incident-field amplitudes has a zero determinant. In so far as the diffracted amplitudes are inversely proportional to this determinant, they have a singularity, i.e., a complex pole. In general, the pole is equal to the guided-wave propagation constant. Because of energy-balance and continuity requirements, this pole must be accompanied by a zero of the amplitudes of the propagating diffraction orders. The values of the poles and the zeros are complex, and their positions in the complex plane depend on grating parameters but not on the angle of incidence.

The phenomenological approach (as well as grating anomalies, in general) has been the subject of extensive studies. Several reviews[4,5] can be found that describe this approach and show how to use its results for predicting the behavior of anomalies. An extension of the formalism[6] shows that the poles and the zeros exist in nonlinear second-harmonic generation by diffraction gratings. Recently the subject was again revived[7,8] in connection with dielectric-grating anomalies when such gratings are used as narrow-band optical filters. In brief, when a waveguide mode is excited in a dielectric grating (usually a corrugated waveguide) the pole leads to a peak and the zero to a dip in the diffraction efficiency and, in particular, in the reflectivity and the transmittivity of the device. When the overall (nonresonant) reflectivity is low the high (theoretically 100%) and narrow peak in the reflectivity can be used for wavelength filtering. In so far as the propagation constants of the guided wave of different polarizations are different, the position of the peak depends strongly on the polarization; thus the filtering properties are polarization selective.

However, experiments have shown that the maximum is quite far from the desired 100%.[8,9] Recently, Magnusson *et al.*[10] achieved a maximum value of 94% but by using a wider-band resonance filter with an angular full width of 12°. The role of losses was treated in detail in Ref. 8 in which a qualitative estimation of the finite-beam-size influence was given, too.

The aim of this paper is to show quantitatively the influence of several observed deviations from the theoretical model on device performance. These deviations include the finite incident-beam width and its divergence and the waveguide losses. We also discuss the influence of the symmetry of the device on its performance, briefly summarizing theoretical research done 15 years ago.[11]

2. MULTILAYER DIELECTRIC-GRATING ANOMALIES

We consider a multilayer dielectric grating that is capable of supporting one or more guided waves. This can be a single-layer corrugated optical waveguide or a multilayer diffraction grating that consists of several corrugated and plane layers. As a result of diffraction by the grating, the

guided wave is radiated into the cladding, the substrate, or both, which introduces radiation losses. Thus its propagation constant becomes complex, and the guided wave is transformed into a leaky one. If a plane wave is incident from the cladding at an angle of incidence θ_i it can excite a guided wave under specific conditions, called the phase-matching or the Bragg condition, given by

$$n_c \sin \theta_i = \frac{\beta_g}{k_0} + m \frac{\lambda}{d}, \tag{1}$$

where n_c is the cladding refractive index, λ is the wavelength, d is the grating period, β_g is the guided-wave propagation constant, $k_0 = 2\pi/\lambda$ (so that β_g/k_0 is the mode effective index), and m is the diffraction order responsible for the excitation (usually equal to -1).

Depending on the λ/d ratio (and on the angle of incidence), several diffraction orders can propagate in the cladding and in the substrate; their amplitudes are denoted by r_m and t_m, respectively. As was discussed in Section 1, in the vicinity of the guided-wave excitation [Eq. (1)] these amplitudes have a pole and zeros. If we assume that the resonance is simple, i.e., only a single mode is excited, the propagating-order amplitudes can be expressed as

$$r_m = r_{0,m} \frac{(\alpha - \alpha_m^{r,z})}{(\alpha - \alpha^p)}, \tag{2a}$$

$$t_m = t_{0,m} \frac{(\alpha - \alpha_m^{t,z})}{(\alpha - \alpha^p)}, \tag{2b}$$

where $\alpha = n_c \sin \theta_i$, α_m^z is the zero of the mth amplitude (which is different in reflection and transmission), and α^p is the pole (which is common for all the amplitudes because it is equal to the zero of the determinant of the inverse scattering matrix). If several guided waves are excited several similar terms with poles and zeros exist in Eqs. (2). The coefficients $r_{0,m}$ and $t_{0,m}$ are slowly varying functions and are equal to the nonresonant amplitudes of the diffraction orders. For a lossless dielectric waveguide the energy balance requires that

$$\frac{1}{\beta_0^r} \sum_{m \in U} (\beta_m^r |r_m|^2 + \beta_m^t |t_m|^2) = 1, \tag{3}$$

where

$$(\beta_m^{r,t})^2 = n_{c,s}^2 - \alpha_m^2, \tag{4}$$

with n_s the refractive index of the substrate and U the numbers of propagating orders (it is, in general, different in the cladding than in the substrate).

In experiments scientists are more often interested in the reflectivity measurements. When looking at Eq. (2a) it is evident that the efficiency in order m can vanish at $\alpha = \alpha_m^{r,z}$ if the value of $\alpha_m^{r,z}$ is real. Moreover, the total reflectivity, which is a sum of the efficiencies of all the reflected orders, will be null, provided the zeros $\alpha_m^{r,z}$ of all the orders are equal and real, which can hardly happen. If, on the other hand, high reflectivity is required, then nullifying the transmission is difficult when several diffraction orders are transmitted. Thus it is better to reduce to a minimum the number of propagating orders by a decrease in the groove period. This is why in the rest of the paper we discuss the case in which only specular orders are reflected and transmitted. Without losses energy conservation requires that the sum of the transmitted-order and the reflected-order efficiencies be equal to unity so that, when one of them has a minimum, the other must show a maximum. The polarization throughout the rest of the paper is taken to be TE (or P or s) polarization with the electric field vector parallel to the grooves, although the results can be generalized directly for the TM case.

3. SYMMETRY CONSEQUENCES

If the zero $\alpha_0^{t,z}$ of the specular transmitted order is real the respective efficiency will be null at an angle of incidence corresponding to this zero:

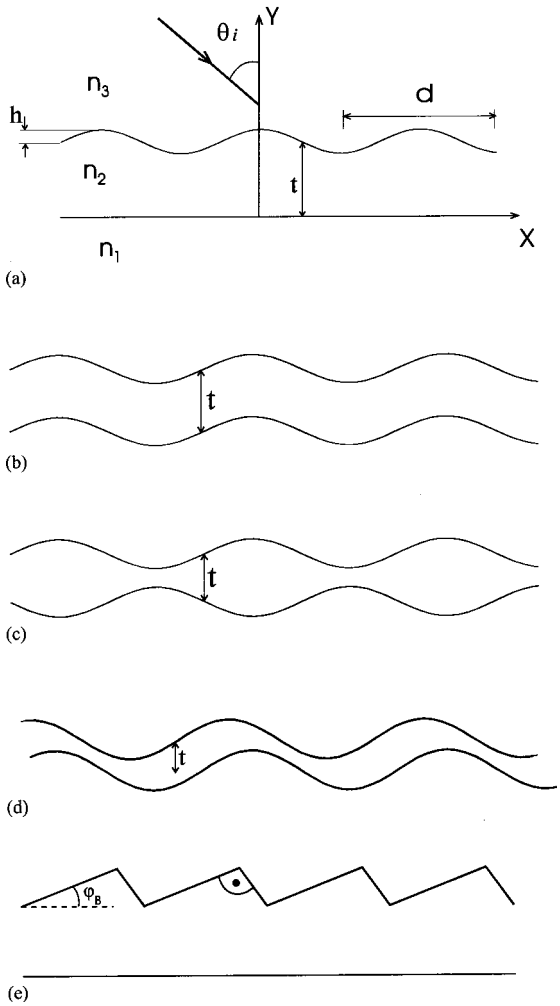

Fig. 1. Schematic representations of different types of corrugated waveguides together with some notation used in the text: d is the groove period, h is the total groove depth, and t is the dielectric-layer thickness. (a) The flat lower interface and the symmetrically corrugated upper interface. (b) Identical corrugations of the two interfaces of (a). The corrugations have symmetry with respect to a vertical plane. When $n_1 = n_3$ the waveguide has an axis of symmetry. (c) The corrugations of (b) but with a horizontal shift of $d/2$; the waveguide has a vertical plane of symmetry. When $n_1 = n_3$ the waveguide has a horizontal plane of symmetry. (d) A horizontal shift between identical corrugations of $d/4$; neither type of symmetry exists. (e) An echelette grating as the upper interface; neither type of symmetry exists.

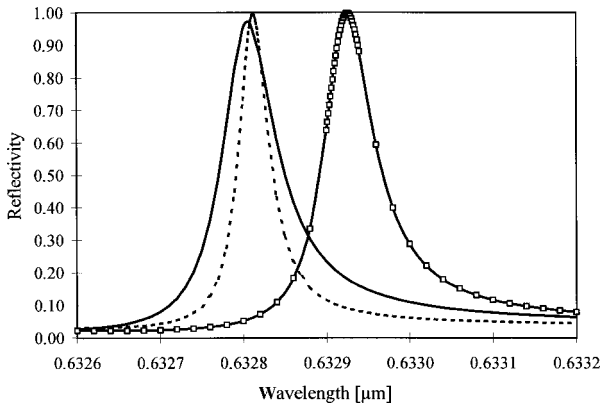

Fig. 2. Spectral dependence of the reflectivity of three corrugated waveguides with identical parameters but with different corrugations. Parameters: TE polarization, $d = 0.303\,\mu$m, $t = 0.7\,\mu$m, $h = 0.12\,\mu$m, $n_1 = 1.5115$, $n_2 = 1.542$, $n_3 = 1$, and $\theta_i = 34.785°$. The solid curve with markers represents the waveguide shown in Fig. 1(a); the dashed curve corresponds to the geometry presented in Fig. 1(c); the plain solid curve represents the grating shown in Fig. 1(d).

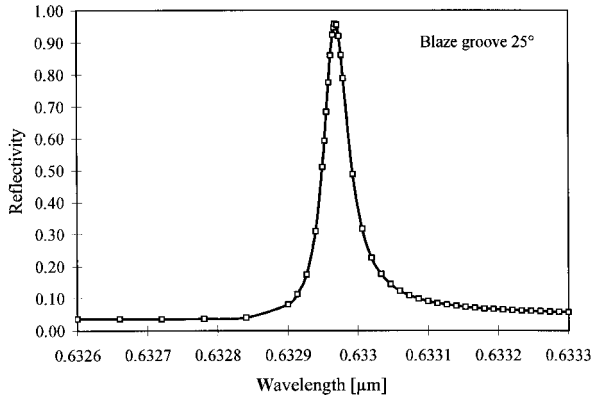

Fig. 3. Spectral dependence of the reflectivity of a corrugated waveguide with a plane as the lower boundary and an echelette as the upper boundary [Fig. 1(e)]. Parameters: TE polarization, $d = 0.303\,\mu$m, $t = 0.65\,\mu$m, $h = 0.12\,\mu$m, $\varphi_B = 25°$, $n_1 = 1.5115$, $n_2 = 1.542$, $n_3 = 1$, and $\theta_i = 34.785°$.

$$\sin\theta_i = \frac{1}{n_c}\alpha_0^{t,z}. \tag{5}$$

If $\alpha_0^{t,z}$ is complex (as it is, in general) the transmission is not null and depends on the ratio of the imaginary parts of the zero and the pole as a consequence of Eq. (2b) when their real parts are close in value:

$$\min(t_0) \propto \frac{\mathrm{Im}(\alpha_m^{t,z})}{\mathrm{Im}(\alpha^p)}. \tag{6}$$

Thus if the transmission-order zero is real, the theoretical maximum of the reflection order reaches 100%, and it remains lower when the transmission-order zero is complex.

The transmission- and the reflection-order zeros are real or complex depending on the symmetry of the system.[11] Three main cases can be distinguished, as presented in Fig. 1:

(i) A corrugated waveguide that is symmetrical with respect to a vertical plane [Figs. 1(a), 1(b), and 1(c)]. This case includes all waveguides with a symmetrical profile. The transmission zero is always real; thus the reflection maximum is equal to 100% in the lossless case, whereas the reflection minimum is not necessarily null.

(ii) There is symmetry with respect to a horizontal plane [Fig. 1(c)]. This case requires that the waveguide be symmetrical, i.e., the optical indices of the cladding and the substrate are equal. In addition, the corrugation must be made with opposite phases on the two boundaries and is difficult to realize. Both transmission and reflection zeros are real, and the reflectivity exhibits a 100% maximum and a 0% minimum.

(iii) There is symmetry with respect to an axis, which acts as a center of inversion in the waveguide cross sec-

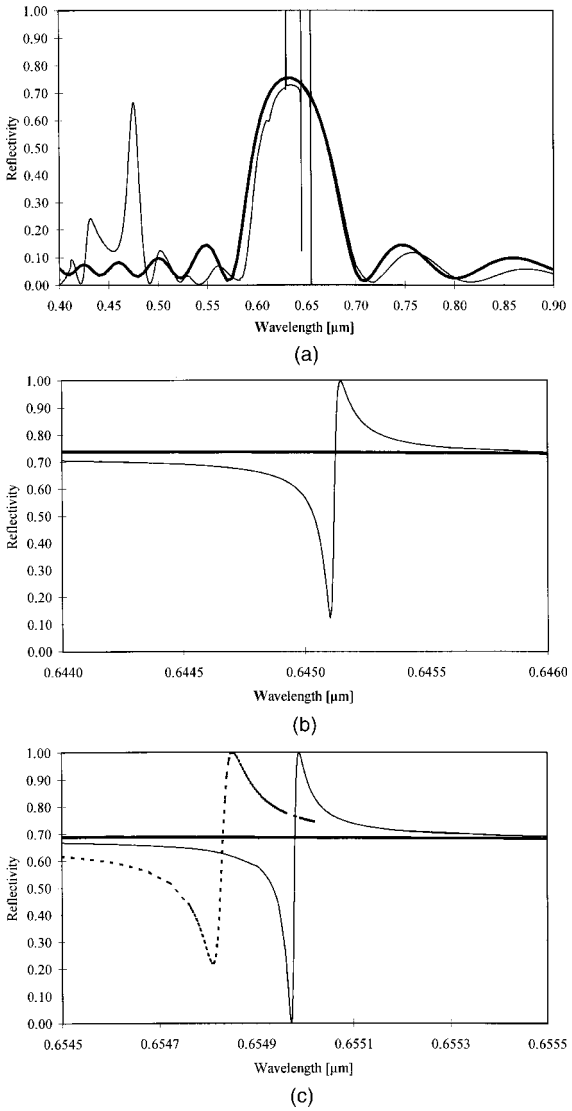

Fig. 4. Spectral dependence of the reflectivity of a multilayer dielectric mirror that consists of 17 layers of dielectrics with alternating higher ($n = 1.7$) and lower ($n = 1.5$) refractive indices. Each layer has a $\lambda/4$ thickness at $\lambda = 0.63\,\mu$m. There is normal incidence and TE polarization. The thick solid curve represents a plane as the upper interface; the thin solid curve represents an upper interface that has a sinusoidal modulation with a period of $d = 0.4117\,\mu$m and a modulation depth of $h/d = 0.2$; the dashed curve represents a case with a 2× modulation rate of $h/d = 0.4$. Shown are (a) the general view, (b) the zoom around the region $\lambda = 0.645\,\mu$m, and (c) the zoom around $\lambda = 0.655\,\mu$m.

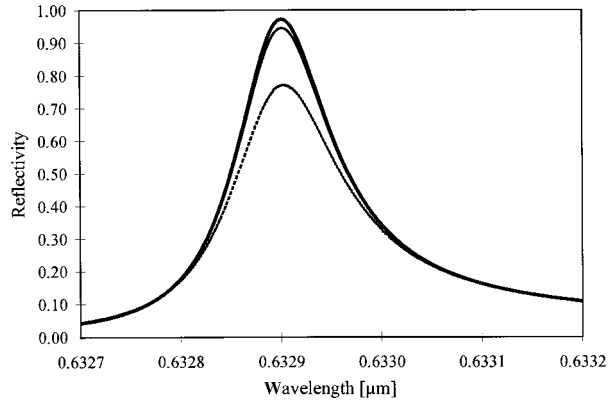

Fig. 5. Spectral dependence of the reflectivity of the corrugated waveguide shown in Fig. 1(b) with TE polarization, $d = 0.303\,\mu$m, $t = 0.7\,\mu$m, $h = 0.12\,\mu$m, $n_1 = 1.5115$, $n_2 = 1.542 + i\gamma$, $n_3 = 1$, and $\theta_i = 34.785°$. The three curves are calculated for different losses in the middle guiding layer that correspond to different values of the extinction coefficient γ. The thick solid curve represents $\gamma = 5 \times 10^{-6}$; the thin solid curve represents $\gamma = 10^{-5}$; the dashed curve represents $\gamma = 5 \times 10^{-5}$.

tion [Fig. 1(b)]. The corrugations must be identical and in phase at the two boundaries, and the substrate and the cladding must have the same indices. The reflection zero is real, which ensures a 100% transmission maximum but does not guarantee 100% reflectivity, as the transmission zero could be complex.

As can be observed, for practical purposes it is the first type of symmetry that has the greatest importance. It means, in particular, that, for all waveguides with symmetrical corrugation on only one of the interfaces, the excitation of a guided wave will lead to a resonance anomaly with a 100% reflectivity maximum, provided there are only specular orders propagating in the cladding and the substrate.

Several numerical examples are presented in Figs. 2 and 3 and point out that, even for waveguides with another type of symmetry, the imaginary part of the transmission zero remains small. Thus the reflectivity maximum is only slightly reduced from 100%.

Another interesting example concerns a diffraction grating placed on a multilayer stack of quarter-wavelength layers with alternating high and low indices to increase the reflectivity. It is well known that such layers form a reflection bandwidth filter, recently called a photonic bandgap in transmission [Fig. 4(a), the thick curve]. Imposing a diffraction grating on such a flat planar structure could result in the formation of defects in the bandgap [Fig. 4(a), the thin curve]. From the point of view taken in this paper such defects are nothing but the resonance anomalies that are due to the excitation of guided waves in the multilayer structure.[12] Because such a thick structure supports many modes, three anomalies, each consisting of a peak and a dip, are visible that are due to the excitation of three different waveguide modes. Contrary to the cases presented in Fig. 2, here the enhanced transmission rather than the enhanced reflection matters. In the gap the nonresonant reflectivity of the system is high, as is expected, so that the resonance anomaly has more-pronounced dips in the reflectivity that are due to the zero of the reflection order. The system symmetry (with respect to a vertical plane) ensures that the transmission zeros are real; thus the maxima of the reflectivity reach the theoretical value of 100%. However, this symmetry does not require that the reflectivity zeros be real and, as can be concluded from Fig. 3, they are not except for the one in the region farthest to the right [Fig. 4(c)]. However, in this case the minimum reflectivity also increases when the groove depth of the overcoating grating is doubled, as can be observed from Fig. 4(c).

4. INFLUENCE OF LOSSES

Unfortunately, all the results given in Section 3, as well as the theoretical considerations[11] that led to conclusions (i)–(iii), are valid only if the waveguide material and the substrate are lossless and the incident wave is a plane wave. However, in practice, neither is the incident beam infinitely wide, nor is it absolutely collimated, nor is the waveguide material lossless. How these factors affect experimentally the reflectivity maximum can be observed in Fig. 9 (below) as well as from Ref. 9. Although the position and the form of the anomaly in the angular and the spectral dependencies of the reflectivity correspond to theoretical predictions, the results are quite far from the theoretically expected 100% maximum.

Figure 5 presents theoretical results showing the influence of losses in the guiding layer. It must be pointed out that the extinction coefficient of $\gamma = 10^{-5}$ means that the waveguide-mode intensity will attenuate 10 times along a propagation distance of 11 mm because the intensity varies in the x direction as $\exp(-2k_0\gamma x)$. Such strong attenuation is not typical of most waveguides and, moreover, is not enough to explain the reduction of the maximum to as low as 75% or 35%, as was reported experimentally.

5. INFLUENCE OF BEAM DIVERGENCE AND LIMITED SIZE

The reason for the influence of deviations from the incident plane wave on the maximum value of the reflectivity lies in the resonant nature of the anomaly, as expressed by Eq. (1). The narrower the anomaly, the greater the influence of the fact that the incident field contains an interval of angles of incidence because each one of its components will generate a response with a spectral maximum situated at different wavelengths, as given by Eq. (1). As a rule of thumb the incident-beam divergence must be much less than the angular width of the resonance.[8] Figure 6 illustrates the effects of these considerations on the example of Sections 2 and 3. Three very close incidence angles (a difference of 0.6 mrad) yield spectral responses in which the maxima overlap only partially so that, when the beam divergence is greater, one can expect a large deterioration in performance, as is shown below.

There is a direct link between the limited beam size and its divergence. Thus, in this section, we investigate only the influence of the incident-beam divergence. Indeed, the incident-beam field E_z^i can be represented as a

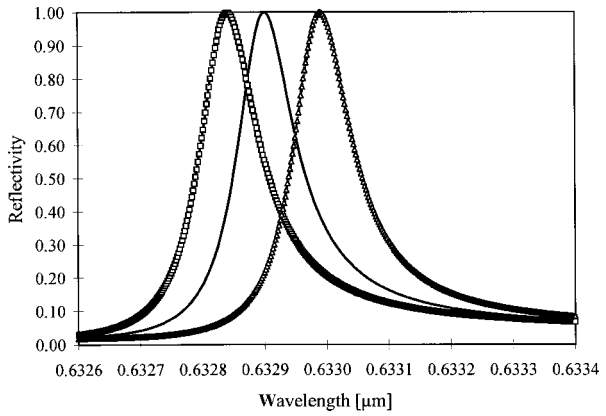

Fig. 6. Spectral dependence of the reflectivity of a lossless waveguide with the parameters of Fig. 5 for three different angles of incidence: $\theta_i = 34.806°$ (triangles), $\theta_i = 34.785°$ (plain curve), and $\theta_i = 34.771°$ (squares).

Fourier transform containing a set of incident plane waves that have some angular distribution $p(\delta)$

$$E_z^i(x,y) = \int_{-\infty}^{+\infty} p(\delta)\exp[i(\alpha x - \beta^r y)]\mathrm{d}\delta, \qquad (7)$$

where δ is equal to α/k_0 and β^r is given in Eq. (4). An incident plane wave has an angular distribution that is equal to the Dirac delta function. In what follows, we assume a Gaussian beam profile with a center at some angle of incidence θ_i such that $\delta_0 = \sin\theta_i$:

$$p(\delta) = \exp\left[-\left(\frac{\delta - \delta_0}{\Delta}\right)^2\right]. \qquad (8)$$

Here, Δ is a dimensionless parameter representing the beam divergence. The smaller Δ is, the less divergent is the incident beam. Typical values for commercial He–Ne lasers vary largely from 0.1 mrad (rarely) to as high as 1 mrad, although laboratory investigations show large deviations from the specified data, usually in the undesired direction.

The linearity of the problem leads to a system response that is a linear combination of responses to each of the incident-field components. Thus the z component of the reflected electric field E_z^r is given by

$$E_z^r(x,y) = \int_{-\infty}^{+\infty} r(\delta)p(\delta)\exp[i(\alpha x + \beta^r y)]\mathrm{d}\delta, \qquad (9)$$

where $r(\delta)$ is the reflection coefficient (with regard to the field amplitude) of the system at an incident angle θ such that $\delta = \sin\theta$.

The diffraction efficiency in the zeroth reflected order (i.e., system reflectivity) is defined as the energy flow in the reflected beam through a plane parallel to the x–z plane and divided by the energy flow of the incident beam through the same surface. Considerations, given in Appendix A, show that the efficiency (reflectivity) η_0 is given by

$$\eta_0 = \frac{\int_{-\infty}^{+\infty} |r(\delta)p(\delta)|^2\beta^r(\delta)\mathrm{d}\delta}{\int_{-\infty}^{+\infty} |p(\delta)|^2\beta^r(\delta)\mathrm{d}\delta}. \qquad (10)$$

The reflectivity of the corrugated waveguide that is expected to ensure a 100% maximum with an incident plane wave (or a beam collimated to better than 0.01 mrad in this specific case) when the beam divergence Δ takes three values between 0.1 and 1 mrad is presented in Fig. 7. A spectacular reduction of the maximum value (shown in Fig. 8) and a broadening of the curves are observed. It must be repeated that the critical beam-divergence value shown in Fig. 8 depends on the anomaly width, as discussed in Ref. 8. On the other hand, the anomaly width is, in general, proportional to the groove depth squared[11]; thus the shallower the grating, the smaller the anomaly width, and the greater the influence of the incident-beam divergence.

An effort to compare these theoretical results with experimental data was made by use of a dye laser with a relatively high beam divergence (greater than 1 mrad). An ion-exchanged waveguide was prepared[9] in an ion-milled photoresist holographic grating that was transferred onto a glass substrate. The fitting of the theoretical data (Fig. 9) with the maximum value results in the choice of $\Delta = 1.2$ mrad, although the theoretical curve is slightly wider than the experimental one. This difference can be explained by our neglect of the losses in the theoretical results and by our taking into account that the experiment involves a gradient-index waveguide,

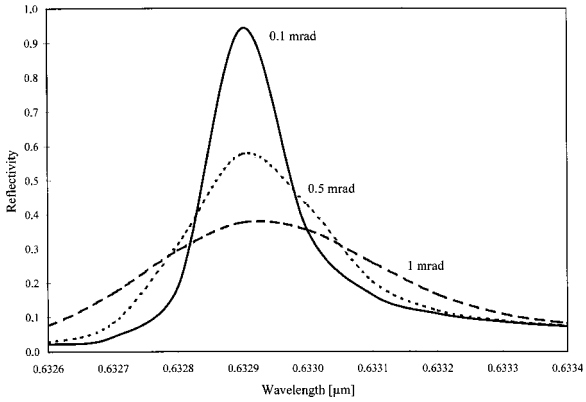

Fig. 7. Spectral dependence of the reflectivity of a lossless waveguide with the parameters of Fig. 5 for three different incident-beam-divergence values. The principal incidence direction is $\theta_i = 34.785°$.

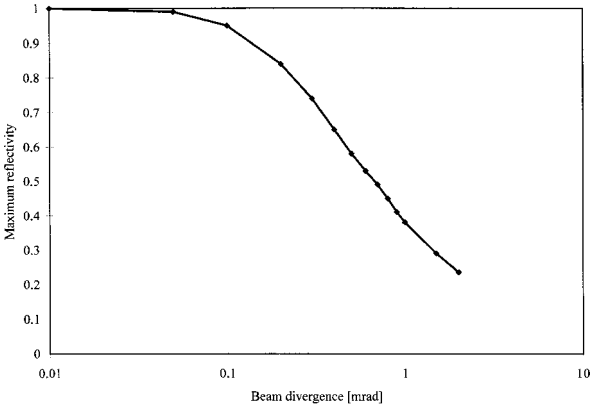

Fig. 8. Values of the reflectivity maxima plotted as a function of the angular beam width. The waveguide parameters are the same as those for Fig. 5.

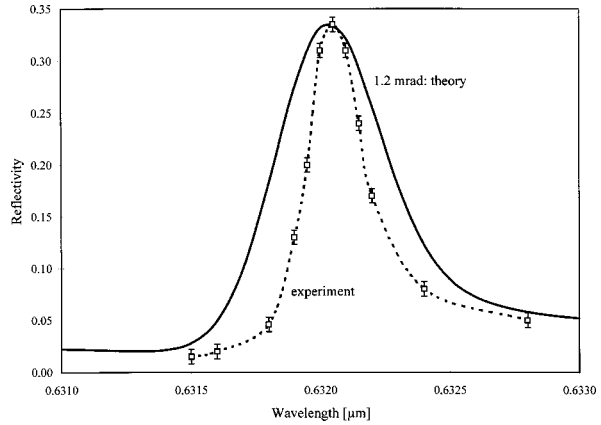

Fig. 9. Comparison of the theoretical and the experimental reflectivities. The theoretical parameters are those given for Fig. 5, and the beam divergence is 1.2 mrad. The experimental values are given in the text.

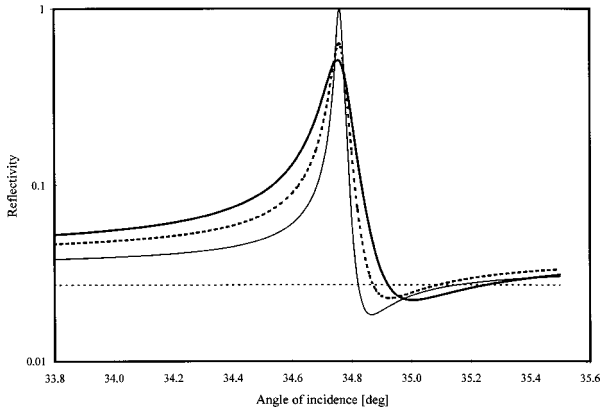

Fig. 10. Angular dependence of the reflectivity of the corrugated waveguide. The thin solid curve represents the theoretical results under the assumption of plane-wave incidence. The thin dashed curve represents the reflectivity of the plane waveguide. The thick dashed curve represents the measurements made with a He–Ne laser with a 0.3-mrad beam divergence. The thick solid curve represents measurements made with the dye laser with a fixed wavelength of 632.8 nm. The logarithmic vertical scale better reveals the form of the anomaly.

whereas the calculations deal with a step-index waveguide. However, this difference is of minor importance to the general conclusion that narrow anomalies, which could be used for narrow-band reflectivity filtering, are quite sensitive to beam collimation, which significantly limits the applications. The role of waveguide losses is not so pronounced, and they have considerable influence on only waveguides with heavy losses, which could be avoided, in practice.

Another measurement was made by use of a second laser with greater beam collimation. A commercial He–Ne laser with a specified divergence of 0.3 mrad was used to measure the angular dependence of the reflectivity of the same corrugated waveguide. A maximum value of 63% was obtained, as compared with the 37% maximum measured with the dye laser. Figure 10 presents a comparison between the theoretically expected results under the assumption of plane-wave incidence and the experimental results obtained with the two lasers. The difference confirms the above conclusions. The use of the logarithmic vertical scale better shows the minimum because of the existence of a zero α^z in Eq. (2a).

APPENDIX A

Let us start with the expressions of the incident- and the reflected-field amplitudes, as given in Eqs. (7) and (9). We are interested in the far-field picture in which these fields are spatially separated. The energy flow through a plane that is parallel to the $x-z$ plane is proportional to the integral along the x axis of the y component P_y of the Poynting vector. For the incident and the reflected beams the energy flow $I^{i,r}$ is proportional to

$$I^{i,r} \propto \int_{-\infty}^{+\infty} P_y^{i,r}(x,y)\big|_{y=\infty} \mathrm{d}x. \tag{A1}$$

The corresponding component P_y is proportional to

$$P_y(x,y) \propto E_z \bar{H}_x \propto E_z \frac{\partial \bar{E}_z}{\mathrm{d}y}, \tag{A2}$$

where the overbar indicates complex conjugation. Taking into account representations (7) and (9) shows that

$$P_y^i(x,y) \propto \int_{-\infty}^{+\infty} \int \mathrm{d}\delta' \mathrm{d}\delta'' p(\delta') \bar{p}(\delta'') \beta'' \times \exp[i(\alpha' - \alpha'')x - i(\beta' - \beta'')x], \tag{A3}$$

$$P_y^r(x,y) \propto \int_{-\infty}^{+\infty} \int \mathrm{d}\delta' \mathrm{d}\delta'' r(\delta') \bar{r}(\delta'') p(\delta') \bar{p}(\delta'') \beta'' \times \exp[i(\alpha' - \alpha'')x - i(\beta' - \beta'')x]. \tag{A4}$$

When expressions (A3) and (A4) are substituted into expression (A1) one of the integrations is eliminated because of the relation

$$\int_{-\infty}^{+\infty} \exp[i(\alpha' - \alpha'')x] \mathrm{d}x = 2\pi\delta(\alpha' - \alpha''), \tag{A5}$$

where, contrary to the rest of the text, δ indicates the Dirac δ function. Then one immediately arrives at Eq. (10).

ACKNOWLEDGMENTS

The authors acknowledge the financial support of the Bulgarian National Foundation of Science of the Ministry of Education and Science under contract 714.

E. Popov's permanent address is the Institute of Solid State Physics, 72 Tzarigradsko Chaussee Boulevard, 1784 Sofía, Bulgaria.

Address correspondence to E. Popov at the address on the title page or e-mail, popov@loe.u-3mrs.fr.

REFERENCES

1. R. Wood, "On a remarkable case of uneven distribution of light in a diffraction grating spectrum," Philos. Mag. **4**, 396–402 (1902).
2. U. Fano, "The theory of anomalous diffraction gratings and

of quasi-stationary waves on metallic surfaces (Sommerfeld's waves)," J. Opt. Soc. Am. A **31**, 213–222 (1941).
3. A. Hessel and A. A. Oliner, "A new theory of Wood's anomalies on optical gratings," Appl. Opt. **4**, 1275–1297 (1965).
4. M. Neviere, "The homogeneous problem," in *Electromagnetic Theory of Gratings*, R. Petit, ed. (Springer-Verlag, Berlin, 1980), Chap. 5.
5. E. Popov, "Light diffraction by relief gratings: a microscopic and macroscopic view," in *Progress in Optics*, E. Wolf, ed. (Elsevier, Amsterdam, 1993), Vol. XXXI, pp. 139–187.
6. M. Neviere, E. Popov, and R. Reinisch, "Electromagnetic resonances in linear and nonlinear optics: phenomenological study of grating behavior through the poles and the zeros of the scattering operator," J. Opt. Soc. Am. A **12**, 513–523 (1995).
7. T. Tamir and S. Zhang, "Resonant scattering by multilayered dielectric gratings," J. Opt. Soc. Am. A **14**, 1607–1616 (1997).
8. S. M. Norton, G. M. Morris, and T. Erdogan, "Experimental investigation of resonant-grating filter line shapes in comparison with theoretical models," J. Opt. Soc. Am. A **15**, 464–472 (1998).
9. L. Mashev and E. Popov, "Zero order anomaly of a dielectric coated grating," Opt. Commun. **55**, 377–380 (1985).
10. R. Magnusson, D. Shin, and Z. S. Liu, "Guided-mode resonance Brewster filter," Opt. Lett. **23**, 612–614 (1998).
11. E. Popov, L. Mashev, and D. Maystre, "Theoretical study of anomalies of coated dielectric gratings," Opt. Acta **33**, 607–619 (1986).
12. L. Mashev and E. Popov, "Diffraction efficiency anomalies of multicoated dielectric gratings," Opt. Commun. **51**, 131–136 (1984).